Collectivity of the pygmy dipole resonance within schematic Tamm-Dancoff approximation and random-phase approximation models

V. Baran,[1] D. I. Palade,[1] M. Colonna,[2] M. Di Toro,[3] A. Croitoru,[1] and A. I. Nicolin[1,4]
[1]*Faculty of Physics, University of Bucharest, Atomistilor 405, Magurele, Romania*
[2]*INFN-LNS, Laboratori Nazionali del Sud, 95123 Catania, Italy*
[3]*Physics and Astronomy Dept., University of Catania, Italy*
[4]*Horia Hulubei National Institute for Physics and Nuclear Engineering, Reactorului 30, Magurele, Romania*
(Received 13 February 2015; revised manuscript received 25 March 2015; published 6 May 2015)

Within schematic models based on the Tamm-Dancoff approximation and the random-phase approximation with separable interactions, we investigate the physical conditions that may determine the emergence of the pygmy dipole resonance in the $E1$ response of atomic nuclei. By introducing a generalization of the Brown-Bolsterli schematic model with a density-dependent particle-hole residual interaction, we find that an additional mode will be affected by the interaction, whose energy centroid is closer to the distance between two major shells and therefore well below the giant dipole resonance (GDR). This state, together with the GDR, exhausts all the transition strength in the Tamm-Dancoff approximation and all the energy-weighted sum rule in the random-phase approximation. Thus, within our scheme, this mode, which could be associated with the pygmy dipole resonance, is of collective nature. By relating the coupling constants appearing in the separable interaction to the symmetry energy value at and below saturation density we explore the role of density dependence of the symmetry energy on the low-energy dipole response.

DOI: 10.1103/PhysRevC.91.054303 PACS number(s): 21.60.Ev, 21.65.Ef, 24.30.Cz

I. INTRODUCTION

In spite of their apparent simplicity, schematic physical models are always very insightful as they provide in a transparent way the essential physical content, which determines a specific feature that is shaping an otherwise complex phenomenon. A quite successful class of such models is that devoted to explain within a quantum many-body treatment the emergence of the collective behavior in various microscopic systems [1], with special emphasis on atomic nuclei [2–5]. To this end, it was pointed out that in the presence of a separable residual particle-hole interaction [6] a coherent superposition of one-particle one-hole states is generated, which carries almost all the transition strength and is pushed up or down in energy from the unperturbed value.

The collectivity of the giant dipole resonance (GDR), one of the most robust modes observed in all nuclei [7], is very well captured in such descriptions [8–12]. As a consequence of the repulsive particle-hole residual interaction, the energy peak gets closer to the empirical mass parametrization, $E_{\mathrm{GDR}} = 80A^{-1/3}$, at almost twice the value associated with the distance between two major shells $\hbar\omega_0 = 41A^{-1/3}$. In recent years experimental investigations [13,14] evidenced the presence of a resonance-shaped state [15–17] below the GDR response but close to the particle threshold energy, exhausting only few percentages of the dipole energy-weighted sum rule (EWSR). The nature of this state is one of the most important open questions in the field and a subject of intense debate [18,19], with current interpretations spanning from a doorway state [20] or single-particle $E1$ strength that fails to join the GDR [21,22], to a collective manifestation of some excess neutrons, which oscillate against the more stable core [23–27]. Moreover, the correlations between the properties of PDR and the behavior of symmetry energy can contribute to constrain the dependence with the density of this quantity [28–30]. It is then natural to ask if schematic models such as those mentioned above are able to provide additional insight about the physical nature of the low-energy dipole response, the role of the symmetry energy, and succeed in the interpretation of the experimentally observed features, such as the energy centroid or the EWSR, when for the parameters of the model realistic values are ascribed, as was the case of GDR.

The purpose of this paper is to investigate the emergence of exotic modes in neutron-rich nuclei and the role of density dependence of the symmetry energy within such schematic models. We shall introduce a generalization of the Brown-Bolsterli schematic model [3,31,32], which admits more general structures for the separable interactions, but which do not spoil the main advantages of the initial model and allow for more general conditions. The coupling constants appearing in these separable interactions will be related not only to the value of symmetry energy at saturation, but some of them are determined by the behavior of this quantity below saturation.

We start with a very brief overview of the schematic approaches, which are relevant for the description of dipole modes. Even if the presentation follows a textbook style, it allows us to introduce those concepts and ideas required for the latter generalizations. Then we analyze possible extensions of these schematic models, based on quite natural physical assumptions, which are able to predict additional collective modes and can incorporate the evolution with density of symmetry energy. As a consequence we can investigate analytically and in a transparent manner how the symmetry energy values at subsaturation density influences the PDR centroid and the sum rules. In the last part we focus on two specific systems, ^{68}Ni and ^{132}Sn, and show that the predictions of these schematic

models agree quite well with data and the results of more sophisticated theoretical approaches. Therefore, we consider that the scenario suggested by our models for the emergence of pygmy dipole resonance as well as that for sharing of the EWSR between PDR and GDR may contribute to a better understanding of the role on symmetry energy on the dynamics of these modes.

For a system of fermions, which interact through an effective two-body potential within a shell-model approach in the absence of ground-state correlations, one usually defines the particle-hole vacuum $|0\rangle$ and the particle (hole) energies associated with the single-particle excitations ϵ_p (ϵ_h).The unperturbed particle-hole excitation energies are obtained as $\epsilon_i = \epsilon_p - \epsilon_h$, where i labels the specific particle-hole configuration. Expressing the interaction among quasiparticles in terms of the difference between direct and exchange terms, as $A_{ij} = \bar{V}_{ph'hp'} = V_{ph',hp'} - V_{ph',p'h} = \langle ph'|\hat{V}|hp'\rangle - \langle ph'|\hat{V}|p'h\rangle$, within the linear approximation of the equations-of-motion method [33], we get the Tamm-Dancoff approximation (TDA) equations:

$$\sum_j (\epsilon_i \delta_{ij} + A_{ij}) X_j^{(n)} = E_n X_i^{(n)}. \tag{1}$$

Together with the normalization condition $\sum_j |X_j^{(n)}|^2 = 1$, Eq. (1) determine the energy E_n of the state $|n\rangle = \Omega^{+(n)}_{\rm TDA}|0\rangle$, as well as the amplitudes, which define the excitation operator:

$$\Omega^{+(n)}_{\rm TDA} = \sum_{p,h} X^{(n)}_{ph} a_p^+ a_h. \tag{2}$$

As a next step, the exchange term is neglected and a separable particle-hole interaction $A_{ij} = \lambda Q_i Q_j^*$ is introduced for the direct one. One then arrives to the dispersion relation:

$$\sum_i \frac{|Q_i|^2}{E_n - \epsilon_i} = \frac{1}{\lambda}, \tag{3}$$

which can be solved for E_n. From a simple graphical analysis one notices that for positive (negative) λ one of the solutions of Eq. (3) is pushed up (down) in energy with respect to the unperturbed energies. This state $|n_c\rangle$ has a collective nature, as it can be easily seen from Eq. (3) if the degenerate case $\epsilon_i = \epsilon$ is considered. Indeed, for this situation the energy of the collective state is given by $E_{n_c} = \epsilon + \lambda \sum_i |Q_i|^2$, while for all others (noncollective) states one finds $E_n = \epsilon$. Moreover, the transition probability $|\langle n_c|Q|0\rangle|^2 = \sum_i |Q_i|^2$, i.e., the collective state exhausts all the energy-independent sum rule, while the transition probability to noncollective p-h states $|n\rangle$ cancels, $\langle n|Q|0\rangle = 0$.

Allowing for correlations in the ground state, the TDA treatment is upgraded to the random phase approximation (RPA). The amplitudes, which appear in the excitation operator

$$\Omega^{+(n)}_{\rm RPA} = \sum_{p,h} X^{(n)}_{ph} a_p^+ a_h + Y^{(n)}_{ph} a_h^+ a_p, \tag{4}$$

and which obey the normalization conditions $\sum_j (|X_j^{(n)}|^2 - |Y_j^{(n)}|^2) = 1$ are obtained from the RPA equations

$$\epsilon_i X_i^{(n)} + \sum_j \left(A_{ij} X_j^{(n)} + B_{ij} Y_j^{(n)}\right) = E_n X_i^{(n)}, \tag{5}$$

$$\epsilon_i Y_i^{(n)} + \sum_j \left(B^*_{ij} X_j^{(n)} + A^*_{ij} Y_j^{(n)}\right) = -E_n Y_i^{(n)}, \tag{6}$$

with $B_{ij} = \bar{V}_{pp'hh'}$. The amplitudes Y_j are a measure of ground-state correlations and by setting all $Y_j = 0$ we recover the TDA equations. For separable particle-hole interactions $A_{ij} = \lambda Q_i Q_j^*$ and $B_{ij} = \lambda Q_i Q_j$ we get the dispersion relation:

$$\sum_i \frac{2\epsilon_i |Q_i|^2}{E_n^2 - \epsilon_i^2} = \frac{1}{\lambda}, \tag{7}$$

which, unlike the TDA treatment, admits a double set of solutions, $\pm E_n$. In the degenerate limit the collective state $|n_c\rangle$ has the energy

$$E^2_{n,\rm RPA} = \epsilon^2 + 2\lambda\epsilon \sum_i |Q_i|^2 = \epsilon(2E_{n,\rm TDA} - \epsilon). \tag{8}$$

A very specific feature of the RPA collective state is that it exhausts the whole EWSR gathered in the unperturbed case, i.e., $E_{n,\rm RPA}|\langle n_c|Q|\tilde{0}\rangle|^2 = \epsilon \sum_i |Q_i|^2$. Here $|\tilde{0}\rangle$ denotes the correlated ground state. Summing up, the residual particle-hole interaction builds up a state, which is a coherent sum of the $|ph\rangle$ states. For a repulsive interaction ($\lambda > 0$), this is characterized by an energy, which is pushed upwards from the unperturbed value and carries all the strength.

The expression of the coupling constant λ can be obtained from considerations based on the self-consistency between the vibrating potential and the induced density variations [34]. In the case of the GDR this quantity is determined by the isovector component of the nuclear interaction, i.e., by the potential contribution to the symmetry energy at saturation. In the expression of the energy per nucleon the symmetry energy $\frac{E_{\rm sym}}{A}$ is the quantity connected to the isospin $I = \frac{N-Z}{A}$ degree of freedom, i.e., $\frac{E}{A}(\rho, I) = \frac{E}{A}(\rho, I=0) + \frac{E_{\rm sym}}{A}(\rho) I^2$ and contains both a kinetic contribution associated with Pauli correlations, as well as a potential contribution determined by the nuclear interaction: $\frac{E_{\rm sym}}{A} = b^{(\rm kin)}_{\rm sym} + b^{(\rm pot)}_{\rm sym}$ [35]. Then $\lambda = \frac{6 b^{(\rm pot)}_{\rm sym}(\rho_0)}{A\langle r^2\rangle}$, where $\langle r^2\rangle$ is the mean-square radius of the nucleus considered and ρ_0 is the saturation density. Considering this value for λ and accounting for the sum rules satisfied by the matrix elements $|Q_i|^2$ [37], the energy centroid and the EWSR exhausted by the GDR were successfully reproduced by the RPA treatment.

II. TDA TREATMENT FOR LOW-LYING MODES

Finite nuclei, however, exhibit a density profile. Since the symmetry energy decreases with density, one expects a smaller value of the coupling constant for the nucleons located at the surface. This is particularly true for neutron-rich nuclei, where several neutrons are located in a region at quite low density, the neutron skin. Analogous arguments

were promoted in phenomenological models [38] when three coupled fluids (i.e., protons, blocked neutrons, and excess neutrons) were considered to describe various normal modes in a hydrodynamical picture. We shall implement this idea in a schematic approach by relaxing the condition of a unique coupling constant for all particle-hole pairs. Similar generalizations of the separable interaction were proposed also in microscopic approaches in order to include the coupling between normal and threshold states [39] or to study the GDR in fissioning nuclei [40]. To this end, we assume that for a subsystem of particle-hole pairs, namely $i,j \leqslant i_c$, the interaction is $A_{ij} = \lambda_1 Q_i Q_j^*$, with $\lambda_1 = \lambda(\rho_0)$ corresponding to the potential symmetry energy at saturation density, while for the other subsystem, namely $i,j > i_c$, the interaction is characterized by a weaker strength $A_{ij} = \lambda_3 Q_i Q_j^*$, with $\lambda_3 = \lambda(\rho_e)$ associated with the symmetry energy value at a much lower density $\rho_e << \rho_0$. If $i \leqslant i_c, j > i_c$ or $i > i_c, j \leqslant i_c$, i.e., for the coupling between the two subsystems, we consider $A_{ij} = \lambda_2 Q_i Q_j^*$ with $\lambda_2 = \lambda(\rho_i)$ corresponding to a potential symmetry energy at an intermediate density $\rho_0 > \rho_i > \rho_e$. As a consequence one of the conditions that the coupling constants will satisfy, obtained from previous physical arguments, is $\lambda_1 > \lambda_2 > \lambda_3 > 0$. The TDA equations for the corresponding amplitudes $X_i^{(n)}$ can be generalized straightforwardly as

$$\epsilon_i X_i^{(n)} + \lambda_1 Q_i \sum_{j\leqslant i_c} Q_j^* X_j^{(n)} + \lambda_2 Q_i \sum_{j>i_c} Q_j^* X_j^{(n)} = E_n X_i^{(n)} \quad \text{if} \quad i \leqslant i_c, \tag{9}$$

$$\epsilon_i X_i^{(n)} + \lambda_2 Q_i \sum_{j\leqslant i_c} Q_j^* X_j^{(n)} + \lambda_3 Q_i \sum_{j>i_c} Q_j^* X_j^{(n)} = E_n X_i^{(n)} \quad \text{if} \quad i > i_c, \tag{10}$$

with the solutions

$$X_i^{(n)} = \frac{N^c}{E_n - \epsilon_i} Q_i \quad \text{if} \quad i \leqslant i_c, \tag{11}$$

$$X_i^{(n)} = \frac{N^e}{E_n - \epsilon_i} Q_i \quad \text{if} \quad i > i_c. \tag{12}$$

Here the normalization factors are given by

$$N^c = \lambda_1 \sum_{j\leqslant i_c} Q_j^* X_j^{(n)} + \lambda_2 \sum_{j>i_c} Q_j^* X_j^{(n)}, \tag{13}$$

$$N^e = \lambda_2 \sum_{j\leqslant i_c} Q_j^* X_j^{(n)} + \lambda_3 \sum_{j>i_c} Q_j^* X_j^{(n)}. \tag{14}$$

Using Eqs. (11)–(14) we observe that N^c and N^e satisfy the homogeneous system of equations:

$$\left(\lambda_1 \sum_{i\leqslant i_c} \frac{|Q_i|^2}{E_n - \epsilon_i} - 1\right) N^c + \lambda_2 \sum_{i>i_c} \frac{|Q_i|^2}{E_n - \epsilon_i} N^e = 0, \tag{15}$$

$$\lambda_2 \sum_{i\leqslant i_c} \frac{|Q_i|^2}{E_n - \epsilon_i} N^c + \left(\lambda_3 \sum_{i>i_c} \frac{|Q_i|^2}{E_n - \epsilon_i} - 1\right) N^e = 0. \tag{16}$$

If we resume to the degenerate case $\epsilon_i = \epsilon$, with $\alpha = \sum_{i\leqslant i_c} |Q_i|^2$, $\beta = \sum_{i>i_c} |Q_i|^2$, by imposing to have nontrivial solutions, we get:

$$(E_n - \epsilon)^2 - (\lambda_1\alpha + \lambda_3\beta)(E_n - \epsilon) + \left(\lambda_1\lambda_3 - \lambda_2^2\right)\alpha\beta = 0. \tag{17}$$

The two states that are affected by interaction in this model will have the TDA energies:

$$E_n^{(1)} = \epsilon + \frac{(\lambda_1\alpha + \lambda_3\beta)}{2}\left(1 + \sqrt{1 - \frac{4\left(\lambda_1\lambda_3 - \lambda_2^2\right)\alpha\beta}{(\lambda_1\alpha + \lambda_3\beta)^2}}\right) \tag{18}$$

$$E_n^{(2)} = \epsilon + \frac{(\lambda_1\alpha + \lambda_3\beta)}{2}\left(1 - \sqrt{1 - \frac{4\left(\lambda_1\lambda_3 - \lambda_2^2\right)\alpha\beta}{(\lambda_1\alpha + \lambda_3\beta)^2}}\right). \tag{19}$$

It is obvious from Eq. (17) that by setting $\lambda_1 = \lambda_2 = \lambda_3 = \lambda$ we return to the standard situation with only one collective energy. Simple expressions for $E_n^{(1)}$ and $E_n^{(2)}$ are obtained if we assume that $\lambda_1\alpha \gg \lambda_3\beta$:

$$E_n^{(1)} \approx \epsilon + (\lambda_1\alpha + \lambda_3\beta), \tag{20}$$

$$E_n^{(2)} \approx \epsilon + \frac{\left(\lambda_1\lambda_3 - \lambda_2^2\right)\alpha\beta}{(\lambda_1\alpha + \lambda_3\beta)}. \tag{21}$$

One of the solutions, $E_n^{(1)}$, is nearest to the value associated with the collective mode obtained in the usual TDA approach while the other one, $E_n^{(2)}$, is much closer to the unperturbed value ϵ. The amplitudes $X_i^{(n_1)}$ and $X_i^{(n_2)}$ will define the two operators whose action on the ground state generates the two states $|n_{c,1}\rangle$ and $|n_{c,2}\rangle$. It is interesting to observe that now energy independent sum rule is distributed only between these two states, i.e.,

$$|\langle n_{c,1}|Q|0\rangle|^2 + |\langle n_{c,2}|Q|0\rangle|^2 = \alpha + \beta = \sum_i |Q_i|^2. \tag{22}$$

We therefore conclude, by extending the interpretation from Brown-Bolsterli model, that both states $|n_{c,1}\rangle$ and $|n_{c,2}\rangle$ manifest the feature expected for a collective behavior. Equation (22) can be easily derived observing that

$$\langle n_{c,k}|Q|0\rangle = \sum_i Q_i X_i^{(n_k)*} = \frac{\alpha + x_k\beta}{\sqrt{\alpha + x_k^2\beta}}, \tag{23}$$

where $k = 1,2$ and $x_k = [(E_n^{(k)} - \epsilon) - \lambda_1\alpha]/\lambda_2\beta$. When all coupling constants become equal the transition amplitude of the state with higher energy goes to $(\alpha + \beta)$, as expected, exhausting all the sum rule.

III. RPA TREATMENT FOR LOW-LYING MODES

Including the ground state correlations does not change the main conclusions obtained within the TDA treatment. Also in this case we shall find the appearance of a second collective state if the unique coupling constant condition is relaxed. The

equations for forward and backward amplitudes become

$$\epsilon_i X_i^{(n)} + \lambda_1 Q_i \left(\sum_{j\leqslant i_c} Q_j^* X_j^{(n)} + \sum_{j\leqslant i_c} Q_j Y_j^{(n)} \right) + \lambda_2 Q_i \left(\sum_{j>i_c} Q_j^* X_j^{(n)} + \sum_{j>i_c} Q_j Y_j^{(n)} \right) = E_n X_i^{(n)}$$

$$\epsilon_i Y_i^{(n)} + \lambda_1 Q_i^* \left(\sum_{j\leqslant i_c} Q_j^* X_j^{(n)} + \sum_{j\leqslant i_c} Q_j Y_j^{(n)} \right) + \lambda_2 Q_i^* \left(\sum_{j>i_c} Q_j^* X_j^{(n)} + \sum_{j>i_c} Q_j Y_j^{(n)} \right) = -E_n Y_i^{(n)}$$

$$\text{if} \quad i \leqslant i_c, \tag{24}$$

$$\epsilon_i X_i^{(n)} + \lambda_2 Q_i \left(\sum_{j\leqslant i_c} Q_j^* X_j^{(n)} + \sum_{j\leqslant i_c} Q_j Y_j^{(n)} \right) + \lambda_3 Q_i \left(\sum_{j>i_c} Q_j^* X_j^{(n)} + \sum_{j>i_c} Q_j Y_j^{(n)} \right) = E_n X_i^{(n)}$$

$$\epsilon_i Y_i^{(n)} + \lambda_2 Q_i^* \left(\sum_{j\leqslant i_c} Q_j^* X_j^{(n)} + \sum_{j\leqslant i_c} Q_j Y_j^{(n)} \right) + \lambda_3 Q_i^* \left(\sum_{j>i_c} Q_j^* X_j^{(n)} + \sum_{j>i_c} Q_j Y_j^{(n)} \right) = -E_n Y_i^{(n)}$$

$$\text{if} \quad i > i_c, \tag{25}$$

with the solutions

$$X_i^{(n)} = \frac{M^c}{E_n - \epsilon_i} Q_i; \quad Y_i^{(n)} = -\frac{M^c}{E_n + \epsilon_i} Q_i^* \quad \text{if} \quad i \leqslant i_c, \tag{26}$$

$$X_i^{(n)} = \frac{M^e}{E_n - \epsilon_i} Q_i; \quad Y_i^{(n)} = -\frac{M^e}{E_n + \epsilon_i} Q_i^* \quad \text{if} \quad i > i_c. \tag{27}$$

The normalization factors

$$M^c = \lambda_1 \sum_{j\leqslant i_c} \left(Q_j^* X_j^{(n)} + Q_j Y_j^{(n)} \right) + \lambda_2 \sum_{j>i_c} \left(Q_j^* X_j^{(n)} + Q_j Y_j^{(n)} \right), \tag{28}$$

$$M^e = \lambda_2 \sum_{j\leqslant i_c} \left(Q_j^* X_j^{(n)} + Q_j Y_j^{(n)} \right) + \lambda_3 \sum_{j>i_c} \left(Q_j^* X_j^{(n)} + Q_j Y_j^{(n)} \right) \tag{29}$$

satisfy the homogeneous system of equations:

$$\left(\lambda_1 \sum_{i\leqslant i_c} \frac{2\epsilon_i |Q_i|^2}{E_n^2 - \epsilon_i^2} - 1 \right) M^c + \lambda_2 \sum_{i>i_c} \frac{2\epsilon_i |Q_i|^2}{E_n^2 - \epsilon_i^2} M^e = 0, \tag{30}$$

$$\lambda_2 \sum_{i\leqslant i_c} \frac{2\epsilon_i |Q_i|^2}{E_n^2 - \epsilon_i^2} M^c + \left(\lambda_3 \sum_{i>i_c} \frac{2\epsilon_i |Q_i|^2}{E_n^2 - \epsilon_i^2} - 1 \right) M^e = 0. \tag{31}$$

In the degenerate case, $\epsilon_i = \epsilon$, nontrivial solutions are obtained if

$$\left(E_n^2 - \epsilon^2\right)^2 - 2\epsilon(\lambda_1\alpha + \lambda_3\beta)\left(E_n^2 - \epsilon^2\right) + 4\epsilon^2\left(\lambda_1\lambda_3 - \lambda_2^2\right)\alpha\beta = 0. \tag{32}$$

Then the collective RPA energies are:

$$E_{n,\mathrm{RPA}}^{(1)2} = \epsilon^2 + 2\epsilon\left(E_{n,\mathrm{TDA}}^{(1)} - \epsilon\right) = \epsilon\left(2E_{n,\mathrm{TDA}}^{(1)} - \epsilon\right), \tag{33}$$

$$E_{n,\mathrm{RPA}}^{(2)2} = \epsilon^2 + 2\epsilon\left(E_{n,\mathrm{TDA}}^{(2)} - \epsilon\right) = \epsilon\left(2E_{n,\mathrm{TDA}}^{(2)} - \epsilon\right), \tag{34}$$

where $E_{n,\mathrm{TDA}}^{(1)}$ and $E_{n,\mathrm{TDA}}^{(2)}$ are the corresponding energies in the TDA approximation given by (18), (19). It is interesting to notice that within the RPA treatment the total EWSR is shared only by these two states, i.e.,

$$E_{n,\mathrm{RPA}}^{(1)} |\langle n_{c,1}|Q|\tilde{0}\rangle|^2 + E_{n,\mathrm{RPA}}^{(2)} |\langle n_{c,2}|Q|\tilde{0}\rangle|^2 = \sum_i \epsilon |Q_i|^2, \tag{35}$$

therefore both of them manifest a collective nature. The last relation can be easily deduced observing that ($k = 1,2$)

$$\begin{aligned} \langle n_{c,k}|Q|\tilde{0}\rangle &= \sum_i \left(Q_i X_i^{(n_k)*} + Q_i^* Y_i^{(n_k)*} \right) \\ &= \sqrt{\frac{\epsilon}{E_{n,\mathrm{RPA}}^{(k)}}} \frac{\alpha + z_k\beta}{\sqrt{\alpha + z_k^2\beta}}; \\ z_k &= \frac{E_{n,\mathrm{RPA}}^{(k)2} - \epsilon^2}{2\epsilon\lambda_2\beta} - \frac{\lambda_1\alpha}{\lambda_2\beta}. \end{aligned} \tag{36}$$

IV. APPLICATION OF THE SCHEMATIC MODELS TO PYGMY DIPOLE RESONANCE IN ^{68}Ni AND ^{132}Sn

In the following we apply the predictions of the schematic TDA and RPA models to specific nuclear systems, where the appearance of a low-lying strength has been observed in the dipole response. Thus we associate the low-energy collective state discussed above with the pygmy dipole resonance (PDR). Several criteria sustaining at least a certain degree of collectivity of PDR, especially in neutron-rich nuclei, were discussed within various models [41,42]. We employ the EWSR associated with the isovector dipolar field corresponding to the unperturbed case: $m_1 = \hbar\omega_0(\alpha + \beta) = \frac{\hbar^2}{2m}\frac{NZ}{A}$. The

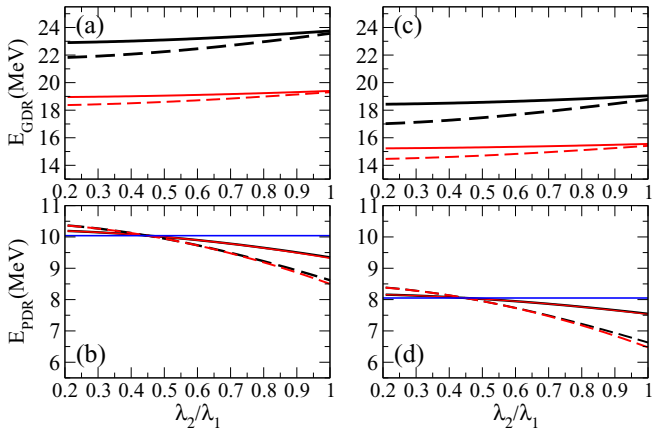

FIG. 1. (Color online) The GDR and PDR energy centroids as a function of the ratio λ_2/λ_1. The black thick lines refer to the TDA while the red lines to RPA calculations. For ^{68}Ni [(a) and (b)] the solid lines correspond to $N_e = 6$; the dashed lines correspond to $N_e = 12$. (b) For ^{132}Sn [(c) and (d)] the solid lines correspond to $N_e = 12$; the dashed lines correspond to $N_e = 32$. In (b) and (d) the horizontal blue line indicates the unperturbed energy value.

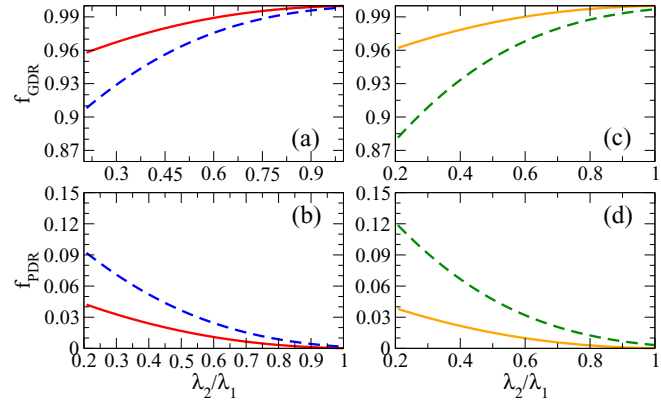

FIG. 2. (Color online) (a) The EWSR fraction exhausted by GDR in RPA calculations for ^{68}Ni. $N_e = 6$ (red solid lines) and $N_e = 12$ (blue dashed lines). (b) The EWSR fraction exhausted by PDR in RPA calculations for ^{68}Ni. $N_e = 6$ (red solid lines) and $N_e = 12$ (blue dashed lines). (c) The EWSR fraction exhausted by GDR in RPA calculations for ^{132}Sn. $N_e = 6$ (orange solid lines) and $N_e = 12$ (blue dashed lines). (d) The EWSR fraction exhausted by PDR in RPA calculations for ^{132}Sn. $N_e = 6$ (orange solid lines) and $N_e = 12$ (green dashed lines).

values for α and β are related to the number of protons (Z_c) and neutrons (N_c), which belong to core, ($A_c = N_c + Z_c$) and the number of neutrons considered in excess, i.e., nucleons at much lower density (N_e), respectively. We first consider N_e as a parameter ($N_e + N_c = N$) but a more precise value can be estimated from arguments based on density distributions of protons and neutrons, as we discuss later. We then obtain $\hbar\omega_0\alpha = \frac{\hbar^2}{2m}\frac{N_c Z}{A_c}$ and $\hbar\omega_0\beta = \frac{\hbar^2}{2m}\frac{N_e Z^2}{A A_c}$ [43,44]. Concerning the coupling constants, we observe that in the presence of the dipolar field the charges of protons and neutrons are considered to be N/A and $-Z/A$, respectively. Then $\lambda_1 = \frac{A^2}{NZ}\frac{10 b_{\rm sym}^{\rm (pot)}(\rho_0)}{AR^2}$, where the nuclear radius is $R = 1.2A^{1/3}$. Let us first adopt for λ_3 a constant value $\lambda_3 = 0.2\lambda_1$, which corresponds to the lower density associated with the neutron skin region and investigate the influence of λ_2 when varied from λ_3 (a weak coupling between the two subsystems) to λ_1 (a strong coupling between the two subsystems).

We consider first the nucleus ^{68}Ni and determine the position of the energy centroid corresponding to the two collective states both in TDA (black thick lines) and RPA (red lines) calculations, see Figs. 1(a), 1(b). Two values were chosen for the number of excess neutrons, namely $N_e = 12$, which corresponds to the extreme case $N_e = N - Z$ (dashed lines) and $N_e = 6$ (solid lines). We observe that the ground-state correlations are influencing strongly the GDR peak and that the RPA predictions are closer to the experimental values (around 17.8 MeV). The PDR energy centroid does not change much either when we modify the value of N_e, nor when we include the ground-state correlations. The experimental value recently reported in Ref. [17] is $E_{\rm PDR}^{\rm exp} = 9.55$MeV, while in our study, for $N_e = 6$, it changes from $E_{\rm PDR} = 10.2$–9.3 MeV, when λ_2 increases from λ_3 to λ_1.

We report the same type of calculations for the ^{132}Sn in Figs. 1(c), 1(d) considering the cases $N_e = 32$ (dashed lines) and $N_e = 12$ (solid lines). For this system, when $N_e = 12$, the position of the PDR energy centroid changes from $E_{\rm PDR} = 8.5 - 7.5$ MeV as λ_2 is varied as before. A steeper decrease is observed for a greater value of N_e. In Fig. 2 we plot the fraction of EWSR exhausted by the GDR ($f_{\rm GDR}$) and the PDR ($f_{\rm PDR}$) as predicted by the RPA calculations for the same systems: ^{68}Ni, Figs. 2(a) and 2(b) and ^{132}Sn, Figs. 2(c) and 2(d). A greater value of N_e determines a larger value of the EWSR fraction exhausted by the PDR. Moreover, $f_{\rm PDR}$ is strongly influenced by the value of the coupling constant λ_2 at variance with the $E_{\rm PDR}$ position. In the case of ^{68}Ni, for $\lambda_2/\lambda_1 = 0.4$, $f_{\rm PDR}$ varies from $2.4 - 5.2$ % when N_e changes from 6 to 12. The experimental values are spanning a domain between 2.8% and 5% [16,17].

For ^{132}Sn in Figs. 3, 4 we represent the global dependence of GDR energy and the EWSR fraction exhausted by GDR

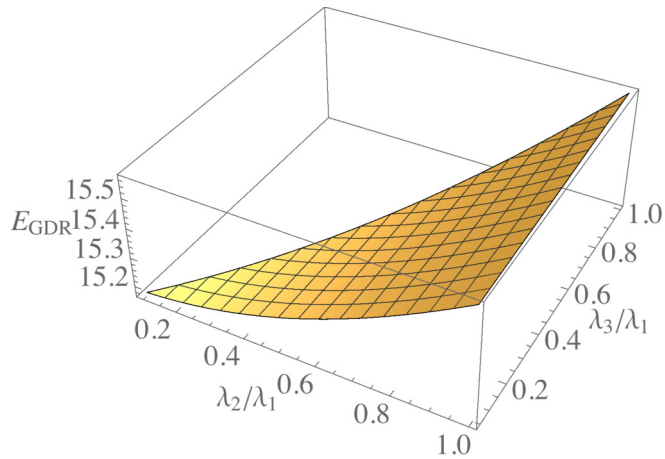

FIG. 3. (Color online) The GDR energy centroids as a function of the ratios λ_2/λ_1, λ_3/λ_1 in the case of ^{132}Sn and $N_e = 13.5$, ($\lambda_2 > \lambda_3$).

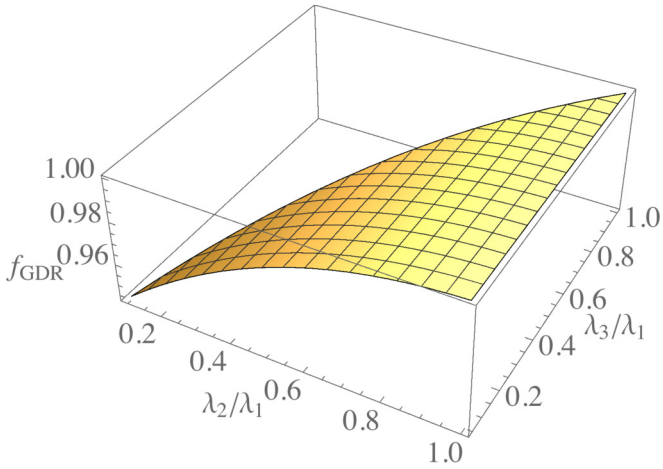

FIG. 4. (Color online) The EWSR fraction ascribed to GDR as a function of the ratios $\lambda_2/\lambda_1, \lambda_3/\lambda_1$ in the case of ^{132}Sn and $N_e = 13.5$, $(\lambda_2 > \lambda_3)$.

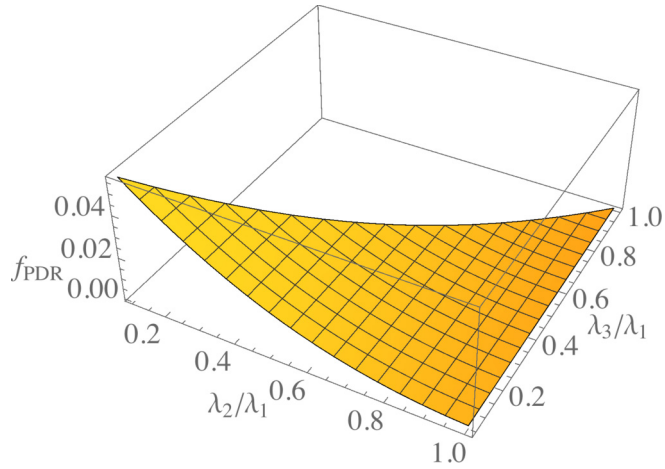

FIG. 6. (Color online) The EWSR fraction ascribed to PDR as a function of the ratios $\lambda_2/\lambda_1, \lambda_3/\lambda_1$ in the case of ^{132}Sn and $N_e = 13.5$, $(\lambda_2 > \lambda_3)$.

as a function of λ_2/λ_1 and λ_3/λ_1 and for $N_e = 13.5$ (see the following discussion, which motivates this choice) derived from the RPA treatment. The same quantities for the PDR are plotted in Figs. 5, 6. We remark that the predictions of the model concerning the position of the two energies are quite robust: one energy is around 15 MeV and the other around 8 MeV and therefore is well suited to describe the two dipole modes observed experimentally in the same energy regions. The predictions are also quite consistent with more complex theoretical approaches for the same nucleus as is relativistic quasiparticle time-blocking approximation [26] or relativistic quasiparticle random phase approximations [45,46]. An important observation that follows from these global plots is a specific sensitivity of the EWSR exhausted by PDR against the values of two parameters λ_2 and λ_3. A stronger coupling between the two subsystems of the model reduces the EWSR ascribed to PDR.

By returning to our discussion concerning the connection between the symmetry energy and these parameters we can adopt now more precise values for them and then compare the predictions of model with data and other theoretical approaches. To analyze the role of the symmetry energy some additional assumptions concerning the connection between the values of λ_i and the density behavior of the symmetry energy are established. Here we employ three different parametrizations of the potential symmetry energy denoted as asysoft, asystiff, and asysuperstiff, respectively [35], which were considered also in the study of PDR in the transport model based on Vlasov equation [44].

The ratio of the coupling constant at a given density ρ to the coupling constant at the saturation density, $\lambda(\rho)/\lambda(\rho_0)$ is shown in Fig. 7 for the three asy-EOS.

We focus our discussion on ^{132}Sn and approximate the radial proton and neutron density distributions by trapezoidal shapes [47]. We reproduce the proton mean-square radius and

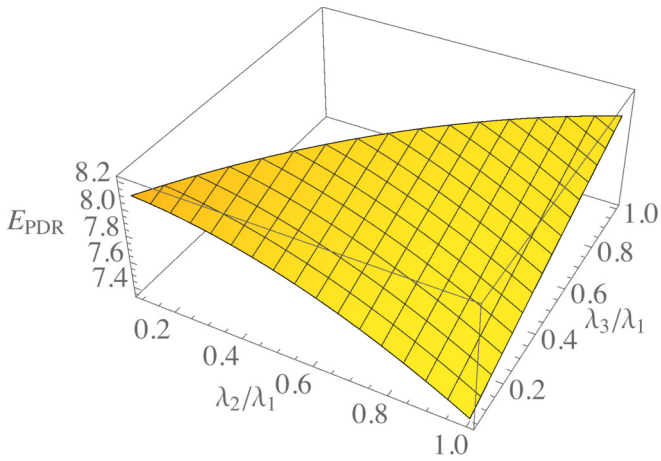

FIG. 5. (Color online) The PDR energy centroids as a function of the ratios $\lambda_2/\lambda_1, \lambda_3/\lambda_1$ in the case of ^{132}Sn and $N_e = 13.5$, $(\lambda_2 > \lambda_3)$.

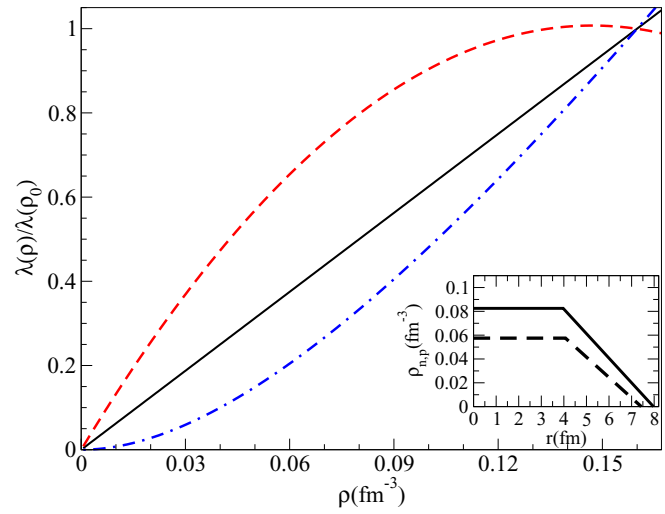

FIG. 7. (Color online) The ratio $\lambda(\rho)/\lambda(\rho_0)$ as a function of density for asystiff EOS (black solid lines), asysuperstiff EOS (blue dot-dashed lines) and asysoft EOS (red dashed lines). The inset: the trapezoidal distribution of neutron (black solid line) and proton (black dashed line) densities for ^{132}Sn considered in the calculations.

TABLE I. The ratios λ_2/λ_1, λ_3/λ_1 corresponding to the realistic physical conditions for the three asy-EOS, the predicted values of PDR, $E_{\rm PDR}$ and GDR, $E_{\rm GDR}$, energy centroids (in MeV), the fraction $f_{\rm PDR}$ exhausted by the PDR in each case. $f^V_{\rm PDR}$ refers to the values obtained from Vlasov calculations.

asy-EoS	λ_2/λ_1	λ_3/λ_1	$E_{\rm PDR}$	$E_{\rm GDR}$	$f_{\rm PDR}(\%)$	$f^V_{\rm PDR}(\%)$
asysoft	0.57	0.23	7.98	15.30	1.3	2.4
asystiff	0.31	0.11	8.05	15.20	3.3	4.2
asysupstiff	0.15	0.02	8.05	15.17	5.0	4.4

obtain a neutron skin thickness $\Delta R_{np} = 0.3$ fm when we adopt for the central densities the values provided by the Vlasov calculations [44], $\rho_n = 0.0825$ fm^{-3}, $\rho_p = 0.0575$ fm^{-3}, see the inset in Fig. 7. We consider the number of neutrons in excess as being determined by the neutron density distribution beyond $r = 6.5$fm, where the tail of the protons distribution is approaching the end part. In this way we obtain a value of N_e around 13.5 neutrons. We also assume that the average density of these particles will define ρ_e, obtaining $\rho_e = 0.0186$ fm^{-3}. For the three asy-EOS we calculate the corresponding λ_3/λ_1 ratio, indicated in Table I. The properties of the region where the total density changes from ρ_0 to zero determine the coupling between the core and the excess neutrons. Therefore we associate the average density of this region with ρ_i, obtaining $\rho_i = 0.05$ fm^{-3}. The corresponding values of the ratio λ_2/λ_1, for the three asy-EOS, are reported in Table I.

With these values of the parameters the PDR energy centroid is found around 8 MeV for all cases. The EWSR fraction exhausted by PDR is strongly influenced by the density dependence of the symmetry energy below saturation. Values equal to 1.3%, 3.3%, and 5.0% are obtained for $f_{\rm PDR}$ when we pass from the asysoft to the superasystiff parametrization. In other words, a stronger coupling between the core and the skin reduces the strength of the PDR response [18], enhancing the GDR contribution. Let us mention that in a transport model based on the Vlasov equation, whose linearized version can be related to the RPA equations [48] and which includes both the isovector and the isoscalar channels of the residual interaction, it was obtained, for ^{132} Sn [49,50], a PDR peak position around 8 MeV, weakly dependent on the asy-EOS, while the EWSR fraction was 2.4%, 4.2%, and 4.4%, for the three symmetry energy parametrizations. Keeping in mind the limits of our assumptions, the agreement between the two models is reasonably good, confirming the clear connection between the behavior of the symmetry energy at quite low densities and the PDR response.

In the present study the influence of the isoscalar component of the residual interaction, which in a neutron-rich system may also affect the isovector response [35,44], is neglected. The mixing of isoscalar and isovector states in the low-lying dipole excitation and the role of neutron skin was investigated for neutron-rich nuclei in Refs. [51,52] within Hartree-Fock plus random phase approximation with Skyrme forces. The study of the evolution of the low-lying dipole strength as the number of neutrons increases [53] indicates a proton contribution to transition density in the nuclear interior and of neutrons at large radii with more collectivity in the heavier isotopes. Moreover, some features of the PDR can only be reproduced going beyond random phase approximation. The coupling of PDR to other surface mode will determine a separation of the PDR into two components, which can be excited by using complementary probes, isoscalar, and isovector respectively [54]. A description of the transition densities based on relativistic quasiparticle time-blocking approximation and a direct comparison with experimental results obtained from inelastic α scattering shows a structural splitting of the low-lying $E1$ strength with an enhanced neutron contribution from the surface and an isoscalar behavior in the nuclear interior [55].

In summary, we introduced in this work schematic models based on separable interactions where the condition of a unique coupling constant for all particle-hole interactions was relaxed. The coupling constant for the isovector dipole response can be related to the potential part of the symmetry energy, which is density dependent and the model is well suited to describe situations when some of the nucleons are located in a region at lower density, as in presence of a neutron skin. Thus, by introducing a density-dependent particle-hole residual interaction for systems with nonuniform density distribution, which generalize the Brown-Bolsterli model, we evidence a mechanism through which the coherent superposition of particle-hole excitations generate two nontrivial states, which are excited by the dipole operator. As a consequence the two collective states will share all the EWSR. The promoted mechanism is supported by the observation that for values of the parameters selected in connection with the features of the symmetry energy below saturation, the predictions of the model agree quite well with more realistic calculations and reproduce simultaneously the basic experimental features of GDR and PDR, which, within this description, appears as a collective mode.

Since the proposed schematic models provide a clear connection between the density dependence of the symmetry energy and the EWSR exhausted by the PDR, we further emphasize that precise experimental determinations of the properties of the low-energy dipole response can settle important constraints on the behavior of the symmetry energy well below saturation.

ACKNOWLEDGMENTS

V.B., A.C., and A.I.N. were supported by a grant from the Romanian National Authority for Scientific Research, CNCS - UEFISCDI, Project No. PN-II-ID-PCE-2011-3-0972. A.I.N. was also supported by the Romanian National Authority for Scientific Research, through the project PN 09370108/2014.

[1] U. Fano, Rev. Mod. Phys. **64**, 313 (1992).
[2] D. M. Brink, Nucl. Phys. A **4**, 215 (1957).
[3] G. E. Brown and M. Bolsterli, Phys. Rev. Lett. **3**, 472 (1959).
[4] N. Vinh-Mau and G. E. Brown, Nucl. Phys. A **29**, 89 (1962).
[5] A. Goswami and M. K. Pal, Nucl. Phys. A **35**, 544 (1962).

[6] G. E. Brown, *Unified Theory of Nuclear Models* (North-Holland, Amsterdam, 1964).
[7] M. N. Harakeh and A. van der Woude, *Giant Resonances* (Clanderon Press, Oxford, 2001).
[8] V. V. Balashov, V. G. Shevchenko, and N. P. Yudin, JETP **41**, 1929 (1961).
[9] V. V. Balashov, Nucl. Phys. A **40**, 93 (1963).
[10] A. M. Green, Prog. Rep. Phys. **28**, 113 (1965).
[11] V. O. Nesterenko, J. Kvasil, and P.-G. Reinhard, Phys. Rev. C **66**, 044307 (2002).
[12] W. Kleinig, V. O. Nesterenko, J. Kvasil, P.-G. Reinhard, and P. Vesely, Phys. Rev. C **78**, 044313 (2008).
[13] T. Aumann and T. Nakamura, Phys. Scr. T **152**, 014012 (2013).
[14] D. Savran, T. Aumann, and A. Zilges, Prog. Part. Nucl. Phys. **70**, 210 (2013).
[15] P. Adrich *et al.*, Phys. Rev. Lett. **95**, 132501 (2005).
[16] O. Wieland *et al.*, Phys. Rev. Lett. **102**, 092502 (2009); O. Wieland, and A. Bracco, Prog. Part. Nucl. Phys. **66**, 374 (2011).
[17] D. M. Rossi *et al.*, Phys. Rev. Lett. **111**, 242503 (2013).
[18] N. Paar, D. Vretenar, E. Khan, and G. Colo, Rep. Prog. Phys. **70**, 691 (2007).
[19] N. Paar, J. Phys. G: Nucl. Part. Phys. **37**, 064014 (2010).
[20] A. M. Lane, Ann. Phys. (NY) **63**, 171 (1971).
[21] B. Gyarmati, A. M. Lane, and J. Zimanyi, Phys. Lett. B **50**, 316 (1974).
[22] L. P. Csernai, J. Zimanyi, B. Gyarmati, and R. G. Lovas, Nucl. Phys. A **294**, 41 (1978).
[23] J. Chambers, E. Zaremba, J. P. Adams, and B. Castel, Phys. Rev. C **50**, R2671 (1994).
[24] D. Vretenar, N. Paar, P. Ring, and G. A. Lalazissis, Nucl. Phys. A **692**, 496 (2001).
[25] M. P. Brine, P. D. Stevenson, J. A. Mahrun, and P.-G. Reinhard, Int. J. Mod. Phys. E **15**, 1417 (2006).
[26] E. Litvinova, P. Ring, V. Tselyaev, and K. Langanke, Phys. Rev. C **79**, 054312 (2009).
[27] E. Yuksel, E. Khan, and K. Bozkurt, Nucl. Phys. A **877**, 35 (2012).
[28] A. Carbone, G. Colò, A. Bracco, L.-G. Cao, P. F. Bortignon, F. Camera, and O. Wieland, Phys. Rev. C **81**, 041301(R) (2010).
[29] M. B. Tsang *et al.*, Phys. Rev. C **86**, 015803 (2012).
[30] L. W. Chen, C. M. Ko, B. A. Li, and J. Xu, Phys. Rev. C **82**, 024321 (2010).
[31] G. E. Brown, L. Castillejo, and J. A. Evans, Nucl. Phys. A **22**, 1 (1961).
[32] G. E. Brown, J. A. Evans, and D. J. Thouless, Nucl. Phys. A **24**, 1 (1961).
[33] T. T. S. Kuo and E. Osnes, in *Collective Phenomena in Atomic Nuclei*, edited by T. Engeland, J. Rekstad, and J. S. Vaagen (International Review of Nuclear Physics, Vol. 2, 1984) p. 79 (World Scientific, Singapore, 1984).
[34] A. Bohr and B. R. Mottelson, in *Nuclear Structure* (World Scientific, Singapore, 1998), Vol. II, p. 481.
[35] V. Baran, M. Colonna, M. Di Toro, and V. Greco, Phys. Rep. **410**, 335 (2005).
[36] Li Bao-An, Lie-Wen Chen, and Che Ming Ko, Phys. Rep. **464**, 113 (2008).
[37] P. Ring and P. Schuck, *The Nuclear Many-Body Problem* (Springer, New York, 1980).
[38] R. Mohan, M. Danos, and L. C. Biedenharn, Phys. Rev. C **3**, 1740 (1971).
[39] H. W. Barz and L. P. Csernai, Nucl. Phys. A **340**, 143 (1980).
[40] P.-G. Reinhard and D. Drechsel, Nucl. Phys. A **295**, 125 (1978).
[41] E. G. Lanza, F. Catara, D. Gambacurta, M. V. Andres, and Ph. Chomaz, Phys. Rev. C **79**, 054615 (2009).
[42] G. Co, V. De Donno, C. Maieron, M. Anguiano, and A. M. Lallena, Phys. Rev. C **80**, 014308 (2009).
[43] V. Baran *et al.*, Rom. J. Phys. **57**, 36 (2012).
[44] V. Baran, B. Frecus, M. Colonna, and M. Di Toro, Phys. Rev. C **85**, 051601(R) (2012).
[45] D. Vretenar, T. Niksic, N. Paar, P. Ring, and Reinhard, Nucl. Phys. A **731**, 281 (2004).
[46] N. Paar, T. Niksic, D. Vretenar, and P. Ring, Phys. Lett. B **606**, 288 (2005).
[47] T. Ikehara and M. Yamada, Prog. Theor. Phys. **71**, 1254 (1984).
[48] B. K. Jennings and A. D. Jackson, Phys. Rep. **66**, 141 (1980).
[49] V. Baran, M. Colonna, M. Di Toro, A. Croitoru, and D. Dumitru, Phys. Rev. C **88**, 044610 (2013).
[50] V. Baran, M. Colonna, M. Di Toro, B. Frecus, A. Croitoru, and D. Dumitru, Eur. Phys. J. D **68**, 356 (2014).
[51] F. Catara, E. G. Lanza, M. A. Nagarajan, and A. Vitturi, Nucl. Phys. A **624**, 449 (1997).
[52] C. H. Dasso, H. M. Sofia, S. M. Lenzi, M. A. Nagarajan, and A. Vitturi, Nucl. Phys. A **627**, 349 (1997).
[53] J. Terasaki and J. Engel, Phys. Rev. C **74**, 044301 (2006).
[54] J. Endres *et al.*, Phys. Rev. Lett. **105**, 212503 (2010).
[55] E. G. Lanza, A. Vitturi, E. Litvinova, and D. Savran, Phys. Rev. C **89**, 041601(R) (2014).